Strategic Backoff of Slotted ALOHA for Minimal Age of Information

Alessandro Buratto[®], *Student Member, IEEE*, Andrea Munari[®], *Senior Member, IEEE*, and Leonardo Badia[®], *Senior Member, IEEE*

Abstract—Random access protocols are usually adopted in the Internet of Things to enable uncoordinated medium sharing. Tackling this setting, we explore the statistics of the packet interdelivery times under slotted ALOHA contention, considering two backoff schemes (reactive vs. proactive). We further discuss the efficiency of these schemes in minimizing the average age of information. Finally, we investigate age minimization both as a centralized optimization and via game theory, obtaining numerical solutions for both cases. A reactive scheme applied in a centralized manner is found to be the most suitable to systems that require a bounded age, whereas a proactive solution applied distributedly is best used to minimize the average age.

Index Terms—Age of information, signal flow graphs, game theory, collision management.

I. INTRODUCTION

RSURING the timeliness of shared information among nodes is critical for effective decision-making in massive distributed scenarios, often encountered in the Internet of things (IoT). Consequently, age of information (AoI) has emerged as a new performance metric [1]. Communication channels in IoT settings are often shared among nodes, and random access solutions based on variations of ALOHA are employed [2]. Moreover, allocating resources individually for each node in a centralized manner may not always be feasible. From this standpoint, game theory is a useful tool to obtain distributed solutions, allowing nodes to make autonomous decisions for optimizing their individual utility, and reducing the overhead needed for network control [3], [4].

Under ALOHA access, simultaneous communication attempts lead to collisions, resulting in the loss of in-flight packets [5], [6]. For this reason, efficient communication protocols aim to mitigate the impact of channel congestion, so as to improve throughput. Under this perspective, the literature proposes many types of countermeasures for issues arising both in collision avoidance and collision resolution

2024; revised 10 October 6 Received November accepted 18 November 2024. Date of publication 22 November 2024; date of current version 10 January 2025. This work was supported by the European Union under the Italian National Recovery and Resilience Plan (NRRP) Mission 4, Component 2, Investment 1.3, CUP C93C22005250001, partnership on "Telecommunications of the Future" (PE00000001 - program "RESTART"), and the Federal Ministry of Education and Research of Germany in the program of "Souveran. Digital. Vernetzt." Joint project 6G-RIC, project identification number: 16KISK022. The associate editor coordinating the review of this letter and approving it for publication was M. C. Lucas-Estany. (Corresponding author: Alessandro Buratto.)

Alessandro Buratto and Leonardo Badia are with the Department of Information Engineering, University of Padova, 35122 Padua, Italy (e-mail: alessandro.buratto.1@phd.unipd.it; leonardo.badia@unipd.it).

Andrea Munari is with the Institute of Communications and Navigation, German Aerospace Center (DLR), 51147 Weßling, Germany (e-mail: andrea.munari@dlr.de).

Digital Object Identifier 10.1109/LCOMM.2024.3504745

[7], [8], but the impact on information freshness is relatively unexplored.

In [9] and [10], AoI was analyzed for different random access protocols, but without considering backoff. Yet, as suggested by [11], there is a basic tradeoff between throughput and delay that can be tuned through the choice of the backoff policy, and since AoI is also somehow mediating between throughput and latency [12], it ought to reflect on that too.

A study that explicitly considers the impact of backoff on AoI is [13], but it only considers a proportional backoff scheme and assumes that the nodes adhere to the same protocol without any strategic planning. Also, [14] proposes three backoff strategies for slotted ALOHA based on random and deterministic approaches and analyzes the optimal and Nash Equilibrium (NE) solutions. Yet, it only considers the average AoI, not discussing other AoI-related metrics.

In this letter, we analyze two backoff strategies in slotted ALOHA: (i) a *proactive* scheme in which nodes enter backoff whenever attempting a transmission regardless of the outcome of the communication attempt and (ii) a *reactive* approach where backoff is undergone only when collision happens.

Our contribution is twofold: firstly, we propose an analysis based on signal flow graphs (SFGs) to obtain closed-form expressions for the average peak AoI (PAoI), the average AoI and the age violation probability. Secondly, we explore the optimization of a metric combining the average AoI and a communication cost, in either a centralized or distributed (i.e., game theoretic) fashion, for both schemes. We discuss the performance in terms of AoI, PAoI, and the age violation probability when fixing a threshold for the peak age.

We find that a reactive scheme is not the best choice to obtain low average AoI values, but an optimal centralized solution that implements it can be suitable to avoid high PAoI. Conversely, a proactive backoff scheme has generally low average AoI, especially if applied in a distributed fashion, but struggles in preventing sudden AoI spikes.

II. SYSTEM MODEL

We consider a discrete time divided into slots. In our scenario, N nodes communicate over a shared channel to a common receiver, sending time-stamped packets following a slotted ALOHA contention. Accordingly, nodes independently transmit in each slot and collisions ensue when the number of accessing nodes is larger than 1. We adopt a collision channel model [2], [5], [6], i.e., the receiver cannot extract information out of a collision, whereas a slot accessed by a single node leads to correct reception. We account for an instantaneous and error-free feedback after each slot to make the nodes aware

of the transmission outcome. We are interested in maintaining information freshness at the receiver. To this end, we compute the instantaneous AoI for node i as the difference between the current time t and the timestamp τ_i of the last correctly received packet sent by that source:

$$\delta_i(t) = t - \tau_i. \tag{1}$$

For age computations, each node always has fresh information (generate-at-will model) as common in the literature [4], [12], and we neglect transmission delays. To capture the long-term performance, we compute the average AoI for node i as

$$\Delta_i = \lim_{T \to \infty} \frac{1}{T} \sum_{t=1}^{T} \delta_i(t). \tag{2}$$

Moreover, we explicitly incorporate a backoff phase to mitigate the effects of collisions. This approach contrasts with most existing studies, where medium access is modeled using an independent and identically distributed (i.i.d.) transmission probability p for each slot [15], [16]. Instead, in our analysis, the nodes switch between an *idle* phase (I) and a *backoff* phase (B), which can be interpreted as states in a Markov chain [5].

We examine two different transition schemes. In each of them, during the idle phase, nodes transmit with i.i.d. probability p. However, they vary in how they handle backoff. The first scheme implements a *Reactive Backoff* (RB): After a collision, a node enters the backoff state, where it remains silent for a random number of slots. This is obtained by setting $a \le 1$ as the probability of going back to idle, leading to a geometric backoff. The second scheme implements a *Proactive Backoff* (PB): Nodes enter backoff after each transmission, regardless of the outcome. Similar to RB, we set a geometric backoff duration with parameter $a \le 1$. This strategy takes inspiration from Threshold ALOHA [17] and it improves on it by applying ideas from collision avoidance.

For both schemes, we describe the state of a node with a discrete time Markov chain (DTMC), whose states I and B correspond to idle and backoff, respectively. State transitions are not memoryless, as the number of nodes in state I directly affects the probability of collisions. However, the steady state probability of the DTMC provides a reasonable approximation, particularly under conditions of large N (e.g., $N \geq 10$) [5].

Each node i independently chooses its own parameters p and a, represented as p_i and a_i . However, for symmetry reasons, both the optimal configuration and the NE will have them converging to the same values across all nodes [14]. If $\pi_I^{(i)}$ and $\pi_B^{(i)}$ are the steady state probabilities that node i is in state I or B, respectively, we have that the transmission probability of node i in the RB and PB schemes is $t_i = \pi_I^{(i)} p_i$.

Successful transmission of node i in a slot depends on that no other node transmits concurrently. Denote the probability of this latter event as $r_i = \prod_{j \neq i} (1-t_j)$ and with $\bar{r}_i = 1-r_i$ its complementary. For PB, t_i admits an exact expression, i.e., $t_i = a_i p_i/(a_i + p_i)$, thereby providing a closed form for r_i . For RB, instead, π_I^i can only be expressed as a recursive function of the steady state probability of each node, such that

$$\pi_I^i p_i \prod_{i \neq i} (1 - \pi_I^j p_j) + a_i - (a_i + p_i) \pi_I^i = 0.$$
 (3)

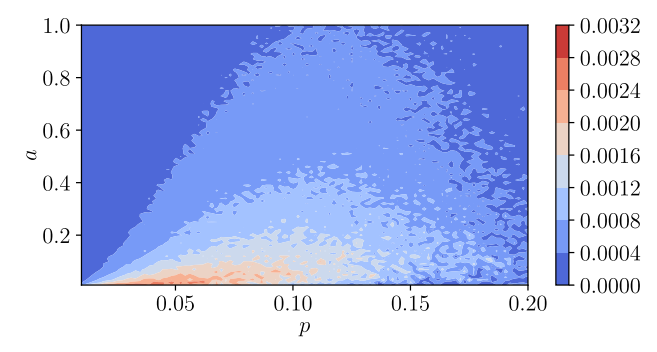


Fig. 1. Difference between the iterative solution for the equation of t_i of RB and a Monte Carlo simulation for N=10 nodes averaging 5 runs with 70000 steps each.

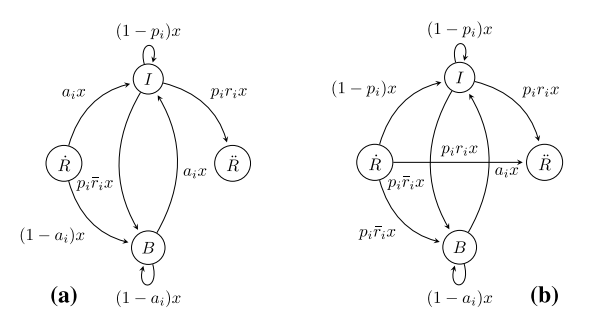


Fig. 2. Signal flow graph for node transitions: PB (a) and RB (b) cases.

Due to the correlated behavior of the nodes relative to collisions, this expression for π_I^i is an approximation for the steady state distribution, but can be shown to be robust in practice. This assertion can be validated through Monte Carlo simulations, as done in the literature for our domain of interest [14]. The result of a simulation for N=10 is reported in Fig. 1.

We characterize the AoI for a generic node i formalizing the DTMCs for PB and RB as signal flow graphs [18]. This allows us to obtain a closed form expression for the probability generating function (PGF) of the inter-update time, denoted as Y. We refer the reader to [19] for more details. To this aim, we modify the original MC by splitting the backoff state for PB and the idle state for RB to include an extra *reset* state. In both cases, the chain transitions to this state whenever the node resets AoI. This state is further divided into \dot{R} (with only outgoing edges) and \ddot{R} (with only incoming edges). The SFG is shown in Fig. 2, where x is a dummy variable multiplying the transition probabilities between states. Leaning on this, a direct application of the Mason's gain formula [18] between \dot{R} and \dot{R} provides the PGF of Y, $G_Y(x) = \mathbb{E}[x^Y]$, not explicitly reported here in the interest of space.

III. AOI CHARACTERIZATION AND NE ANALYSIS

PAoI is the highest AoI reached before a successful transmission. and is commonly used to gauge worst-case system performance. By definition, the average PAoI \mathcal{K}_i for node i is computed as the average of the interupdate times, i.e., [20]

$$\mathcal{K}_i = \mathbb{E}[Y] = G_Y'(1),\tag{4}$$

where $G'_{V}(x)$ denotes the first order derivative of G_{V} with respect to x. For PB and RB, the average PAoI is thus

$$\mathcal{K}_i^{\text{PB}} = \frac{a_i + p_i}{a_i p_i r_i} \tag{5}$$

$$\mathcal{K}_i^{\text{PB}} = \frac{a_i + p_i}{a_i p_i r_i} \tag{5}$$

$$\mathcal{K}_i^{\text{RB}} = \frac{a_i + p_i - p_i r_i}{a_i p_i r_i}. \tag{6}$$

On the other hand, the average AoI can be computed from the first and second order moments of Y [12]. Denoting as $G_Y''(x)$ the second derivative of the PGF, the average AoI is

$$\Delta_i = \frac{\mathbb{E}[Y^2]}{2\mathbb{E}[Y]} = \frac{G_Y''(1) + G_Y'(1)}{2G_Y'(1)} \tag{7}$$

With this formula, we obtain closed form expressions for the average AoI Δ_i^{PB} and Δ_i^{RB} of PB and RB, respectively, as

$$\Delta_i^{\text{PB}} = \frac{a_i^2 (2 - p_i r_i) - a_i p_i [(p_i + 2) r_i - 4] + 2p_i^2}{2a_i p_i r_i (a_i + p_i)},$$
 (8)

$$\Delta_{i}^{PB} = \frac{a_{i}^{2}(2 - p_{i}r_{i}) - a_{i}p_{i}[(p_{i} + 2)r_{i} - 4] + 2p_{i}^{2}}{2a_{i}p_{i}r_{i}(a_{i} + p_{i})},$$

$$\Delta_{i}^{RB} = \frac{a_{i}^{2}(2 - p_{i}r_{i}) + a_{i}p_{i}(r_{i} - 1)(p_{i}r - 4) - 2p_{i}^{2}(r_{i} - 1)}{2a_{i}p_{i}r_{i}(a_{i} - p_{i}r_{i} + p_{i})}.$$
(6)

Finally, through PGF $G_{Y_i}(x)$, a closed form for the probability mass function (PMF) ρ_k of the interarrival times Y_i can also be computed. However, $\rho_k = G_{Y_i}^{(k)}(0)/k!$ is computationally infeasible for an exact expression. An alternative considers the decomposition of the PGF in partial fractions. As $G_{Y_i}(x)$ is rational in the dummy variable x, it can be decomposed into partial fractions with reasonable complexity. The full procedure is described in [21] and applying it to our case leads to the following expressions. For the sake of compactness, let $d = \sqrt{(a_i + p_i)^2 - 4a_i p_i r_i}$, $\xi_j = a_i + p_i - 4a_i p_i r_i$ $(2+(-1)^j d)$ and $\nu_i = a_i - 2p_i r_i + p_i - 1 + (-1)^j d$. For any $\tau \in \mathbb{N}$, the PMF for the interarrival times in PB is

$$\rho_{\tau}^{\text{PB}} = \begin{cases} 0 & if \ \tau = 0 \\ \frac{a_i p_i r_i 2^{-\tau - 1}}{d[a_i (p_i r - 1) - p_i + 1]} & \\ \times \left[\xi_1 \left(-1/\xi_0 \right)^{-\tau} - \xi_0 \left(-1/\xi_1 \right)^{-\tau} \right] & if \ \tau \ge 1 \end{cases}$$

and for RB

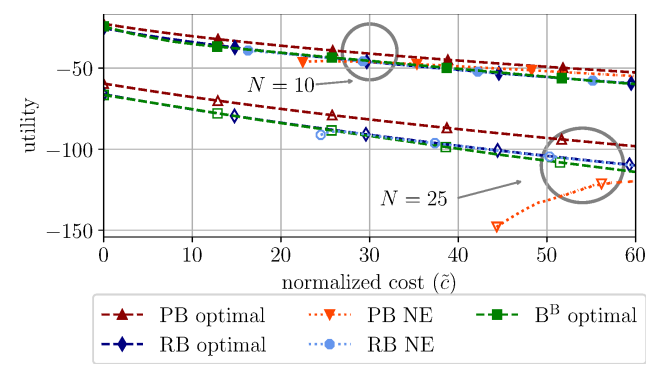
$$\rho_{\tau}^{\text{RB}} = \begin{cases}
0 & if \ \tau = 0 \\
\frac{p_{i}r_{i}2^{-\tau-1} (d-a_{i}\nu_{0}-p_{i}) (-1/\xi_{1})^{-\tau}}{d[a_{i}(p_{i}r-1)-p_{i}+1]} & \\
+\frac{p_{i}r_{i}2^{-\tau-1} (d+a_{i}\nu_{1}+p_{i}) (-1/\xi_{0})^{-\tau}}{d[a_{i}(p_{i}r_{i}-1)-p_{i}+1]} & if \ \tau \geq 1
\end{cases}$$
(10)

With these expressions, we compute the age violation probability, i.e., the probability that at any point in time the AoI exceeds the average PAoI \mathcal{K} :

$$\mathbb{P}[\delta_i > \mathcal{K}] = 1 - \sum_{\tau=0}^{\mathcal{K}} \rho_{\tau}.$$
 (11)

Similar to the literature [4], [6], we consider a cost paid by nodes for every transmission, even if it ends up in a collision. This is captured by coefficient c, which can be connected to energy consumption, or a shadow price to limit the aggressiveness of nodes [16], [22]. The utility of node i is

$$u_i(\mathbf{t}) = -\Delta_i(\mathbf{t}) - ct_i, \tag{12}$$



Expected utility obtained by each node. Full markers for Fig. 3. N=10 nodes, empty markers for N=25 nodes.

meant as an objective that node i seeks to maximize. Vector $t = (t_1, t_2, \dots, t_N)$ collects the N transmission probabilities of all nodes; its best global choice is a symmetrical vector $t^* = (t^*, t^*, \dots, t^*).$

For a distributed solution, we model the problem as a static game of complete information $\mathcal{G} = \{\mathcal{N}, \mathcal{A}, \mathcal{U}\}$ where \mathcal{N} is the set of players, i.e., the nodes, and A is the set of actions available to the nodes, namely, choosing parameters p and a. Finally, \mathcal{U} is the set of utilities as described in (12). The NE for the game \mathcal{G} is derived from each player's unilateral optimization of their utility, meaning that each player seeks a best response to the fixed actions of the other players. For simplicity, we concentrate on player 1. A NE must satisfy

$$\nabla u_1(\mathbf{t}) = \mathbf{0},\tag{13}$$

indicating that the utility's partial derivatives with respect to p_1 and a_1 are zero. In the PB scheme, the partial derivative of the utility with respect to a_1 (the expression for p_1 is analogous with a and p interchanged) can be expressed as

$$\frac{\partial u_1\left(\mathbf{t}\right)}{\partial a_1} = \frac{2a_1p_1 + p_1^2 - a_1^2(r_1 - 1)}{a_1^2r_1(a_1 + p_1)^2} + c\frac{a_1p_1}{(a_1 + p_1)^2} = 0.$$
(14)

For RB similar expressions can be obtained, which are not reported here due to space constraints.

By replacing index 1 with that of a generic player, the expression can be evaluated for all nodes. Remembering the symmetry of the scenario and that acceptable solutions are in the domain of probabilities, we can solve a system of differential equations to obtain the NE, which can be done by numerical means. It is notable that the solutions are symmetrical as in the centralized optimal case, therefore the index i will be omitted for the remainder of this letter.

For small values of c, there is no solution to the system, which means that the only NE is a catastrophic equilibrium, where p = a = 1 for all the nodes. This is undesirable, because the majority of nodes would be constantly colliding or in a backoff state, thus not transmitting. For sufficiently high costs, another more efficient NE appears [4].

IV. NUMERICAL RESULTS

We report numerical evaluations of the derived equations. We use a normalized cost $\tilde{c} = c/N$ to abstract from the number of nodes N. In all the following figures, we set N=10, but Figs. 3 and 5 also plot the results for N=25. To evaluate the

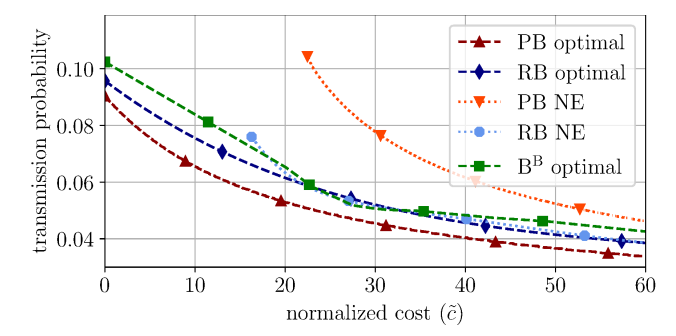


Fig. 4. Transmission probability, N = 10 nodes.

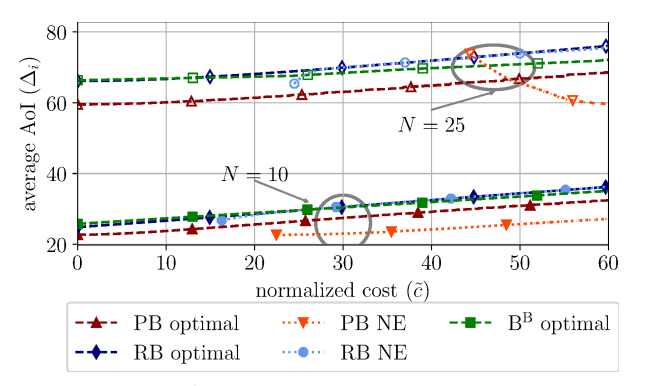


Fig. 5. Average AoI Δ_i . Full markers for N=10 nodes, empty markers for N=25 nodes.

effect of backoff optimization, we simulated, as a benchmark, a non-optimized backoff with binary exponential increase of the contention window. In this binary exponential backoff strategy, denoted as B^B , the optimization is limited to t, chosen so as to maximize utility (12), whereas the backoff follows a procedure similar to IEEE 802.11, i.e., each colliding node retransmits after a number of slots randomly selected within $[2^0, 2^k]$ where $k \in \{1, \ldots, 5\}$ is the number of consecutive collisions [23].

Fig. 3 shows the utility obtained by the different backoff schemes both at the optimum and at the NE. PB obtains the best utility, but the NEs for RB and PB approach the optimal centralized solution for increasing normalized cost. The performance of B^B is similar to RB, which proves that our chosen strategies are meaningful (yet, unlike B^B , they allow for distributed control). A larger number of nodes causes the NE to exist only for higher values of \tilde{c} , in line with the findings of [4]. Interestingly, under RB the NE quickly approaches the optimal solution, whereas, under PB, the NE performance is worse as the nodes transmit more aggressively.

Fig. 4 plots the transmission probability of the nodes either in a centralized configuration, corresponding to the optimization of (12), or at the NE. PB has the lowest centralized transmission probability. This is explained by the conservative approach of this strategy, which undergoes backoff after each transmission. However, limiting the transmission probability also reduces the collision probability when a node eventually makes an attempt. Still, the NE solution has the highest transmission probability, confirming that a distributed approach is actually more aggressive. RB instead has higher transmission probability, since nodes enter a backoff state only after a collision, but the NE converges very rapidly to the optimal value. For higher number

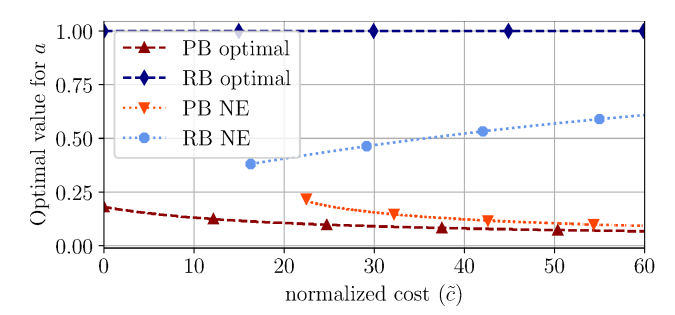


Fig. 6. Backoff exit probability, N = 10 nodes.

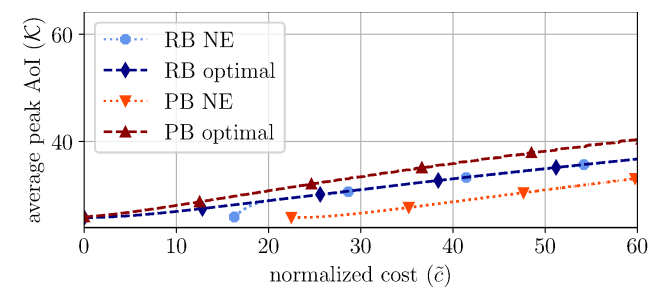


Fig. 7. Average peak AoI, N = 10 nodes.

of nodes N, the trends do not change much and are therefore not reported here.

In Fig. 5, we report the average AoI vs. \tilde{c} , for all backoff schemes. Recall that the optimization goal is not AoI alone, but a linear combination of AoI and transmission cost. The two optimal solutions have similar slope and PB obtains the best values. The lowest average AoI is obtained by PB at the global optimum with $\tilde{c} = 0$ and at the NE for higher costs. This is not in contrast with the results for the utility, as at the NE the nodes transmit more frequently. As for the transmission probability, NE for RB quickly goes towards the optimal solution for increasing cost. For N > 10, the solution trends remain consistent. In both PB and RB, NE solutions occur at higher normalized costs as the network size increases, more notably in PB, indicating its design hinders collaborative behavior. However, the lowest AoI value at NE exceeds the global optimal one at $\tilde{c} = 0$. This plot also shows that B^B is mostly aligned with RB and only takes an advantage in terms of AoI only for very high \tilde{c} and at the expense of higher transmission probability.

Fig. 6 shows the probability a of exiting backoff. The centralized optimal choice for RB is a=1, i.e., each node backs off for one slot and immediately resumes transmission. This aggressive strategy is not employed at the NE, as it would mean that all nodes prefer to be idle, which is the more expensive state when a transmission attempt occurs.

Fig. 7 displays the mean peak AoI \mathcal{K} for the backoff strategies. Interestingly, while optimizing for the average AoI, PB has the highest average peak AoI. This is possibly due to the increased time nodes spend in backoff state. Furthermore, the optimal solutions for PB and RB start from the same point and then have different slopes depending on the backoff strategy. Also in this case, the NE solution for RB approaches the optimal centralized one indicating that also for the peak AoI the most influential parameter is the transmission probability. This difference in performance with respect to the average AoI underlines the importance of choosing the backoff

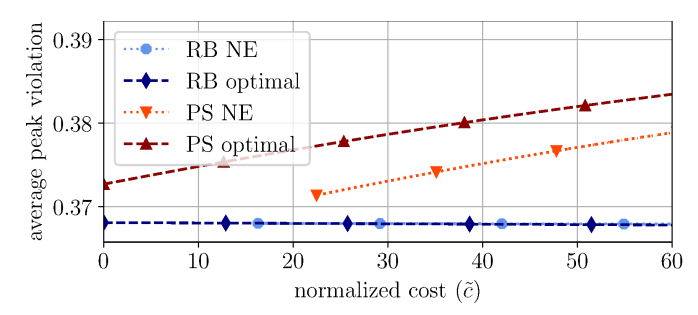


Fig. 8. Average Peak AoI violation probability, N = 10 nodes.

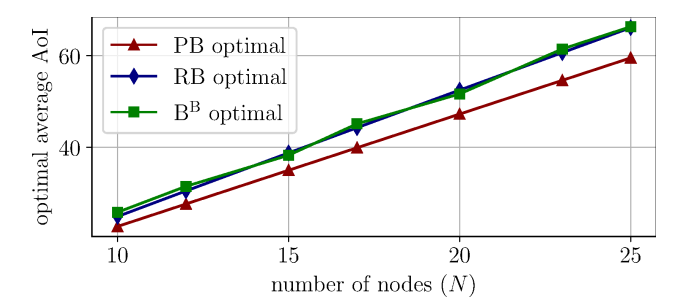


Fig. 9. Optimal value for the considered backoff strategies for $\tilde{c} = 0$.

strategy of the system according to the KPI of interest as PB performs best for the average AoI but not for the average PAoI.

Fig. 8 displays the probability that the AoI violates the average peak AoI values reported in Fig. 7. RB is better at containing the age violation probability than PB both for the optimal solution and for the NE one. This could be explained once again by the similar transmission probability adopted by the method for both solutions. Interestingly, all probabilities are around 38%, implying that the average peak AoI is not a good bound for the robustness of the system when it comes to guaranteeing good quality of service.

Fig. 9 shows the values of AoI for $\tilde{c}=0$ for different number of nodes. It is evident that RB and B^B have similar performance, while PB has incresing advantages as the number of nodes increases. For higher values of the normalized cost, the trends remain the same, but the gap between RB and PB increases superlinearly as hinted in Fig. 5.

V. CONCLUSION

We derived analytical expressions for two backoff strategies in slotted ALOHA, concerning the average AoI, average peak AoI, and PMF of the interarrival times. We also numerically solved an average AoI minimization problem under centralized management, as well as in a distributed way by finding the NEs of a static game of complete information. We argue that a distributed implementation of PB scheme is more efficient at minimizing the average AoI than its competitors, but struggles more at guaranteeing high quality of service when considering peaks in the AoI evolution through time. Similarly, a centralized scheme for RB obtains higher average AoI, but is more resilient to AoI spikes.

REFERENCES

- J. F. Grybosi, J. L. Rebelatto, and G. L. Moritz, "Age of information of SIC-aided massive IoT networks with random access," *IEEE Internet Things J.*, vol. 9, no. 1, pp. 662–670, Jan. 2022.
- [2] M. Noori, S. Rahimian, and M. Ardakani, "Capacity region of Aloha protocol for heterogeneous IoT networks," *IEEE Internet Things J.*, vol. 6, no. 5, pp. 8228–8236, Oct. 2019.
- [3] A. B. MacKenzie and L. A. DaSilva, *Game Theory for Wireless Engineers*. Cham, Switzerland: Springer, 2022.
- [4] L. Badia, A. Zanella, and M. Zorzi, "A game of ages for slotted Aloha with capture," *IEEE Trans. Mobile Comput.*, vol. 23, no. 5, pp. 4878–4889, May 2024.
- [5] G. Bianchi, "Performance analysis of the IEEE 802.11 distributed coordination function," *IEEE J. Sel. Areas Commun.*, vol. 18, no. 3, pp. 535–547, Mar. 2000.
- [6] R. T. B. Ma, V. Misra, and D. Rubenstein, "An analysis of generalized slotted-aloha protocols," *IEEE/ACM Trans. Netw.*, vol. 17, no. 3, pp. 936–949, Jun. 2009.
- [7] Z. Huang et al., "A novel cross layer anti-collision algorithm for slotted ALOHA-based UHF RFID systems," *IEEE Access*, vol. 7, pp. 36207–36217, 2019.
- [8] F. Clazzer, C. Kissling, and M. Marchese, "Enhancing contention resolution Aloha using combining techniques," *IEEE Trans. Commun.*, vol. 66, no. 6, pp. 2576–2587, Jun. 2018.
- [9] X. Chen, K. Gatsis, H. Hassani, and S. S. Bidokhti, "Age of information in random access channels," *IEEE Trans. Inf. Theory*, vol. 68, no. 10, pp. 6548–6568, Oct. 2022.
- [10] A. Munari, "Modern random access: An age of information perspective on irregular repetition slotted Aloha," *IEEE Trans. Commun.*, vol. 69, no. 6, pp. 3572–3585, Jun. 2021.
- [11] X. Sun and L. Dai, "Backoff design for IEEE 802.11 DCF networks: Fundamental tradeoff and design criterion," *IEEE/ACM Trans. Netw.*, vol. 23, no. 1, pp. 300–316, Feb. 2015.
- [12] R. D. Yates, Y. Sun, D. R. Brown, S. K. Kaul, E. Modiano, and S. Ulukus, "Age of information: An introduction and survey," *IEEE J. Sel. Areas Commun.*, vol. 39, no. 5, pp. 1183–1210, May 2021.
- [13] P. Mollahosseini, S. Asvadi, and F. Ashtiani, "Effect of variable backoff algorithms on age of information in slotted Aloha networks," *IEEE Trans. Mobile Comput.*, vol. 23, no. 9, pp. 8620–8633, Sep. 2024.
- [14] A. Buratto and L. Badia, "Analysis of age of information in slotted Aloha networks with different strategic backoff schemes," in *Proc. IEEE* 28th Int. Workshop Comput. Aided Model. Design Commun. Links Netw. (CAMAD), Nov. 2023, pp. 87–92.
- [15] D. C. Atabay, E. Uysal, and O. Kaya, "Improving age of information in random access channels," in *Proc. IEEE INFOCOM Conf. Comput. Commun. Workshops (INFOCOM WKSHPS)*, Jul. 2020, pp. 912–917.
- [16] A. B. MacKenzie and S. B. Wicker, "Selfish users in aloha: A game-theoretic approach," in *Proc. IEEE 54th Veh. Technol. Conf. VTC Fall.*, vol. 3, Aug. 2001, pp. 1354–1357.
- [17] O. T. Yavascan and E. Uysal, "Analysis of slotted ALOHA with an age threshold," *IEEE J. Sel. Areas Commun.*, vol. 39, no. 5, pp. 1456–1470, May 2021.
- [18] S. Mason, "Feedback theory-some properties of signal flow graphs," Proc. IRE, vol. 41, no. 9, pp. 1144–1156, Sep. 1953.
- [19] A. Munari, "On the value of retransmissions for age of information in random access networks without feedback," in *Proc. IEEE Global Commun. Conf. (GLOBECOM)*, Dec. 2022, pp. 4964–4970.
- [20] Y. Khorsandmanesh, M. J. Emadi, and I. Krikidis, "Average peak age of information analysis for wireless powered cooperative networks," *IEEE Trans. Cognit. Commun. Netw.*, vol. 7, no. 4, pp. 1291–1303, Dec. 2021.
- [21] W. Feller, An Introduction To Probability Theory and Its Applications, vol. 1. Hoboken, NJ, USA: Wiley, 1957.
- [22] S. Banerjee, S. Ulukus, and A. Ephremides, "Age of information games between power constrained schedulers and adversaries," *J. Commun. Netw.*, vol. 25, no. 5, pp. 631–642, Oct. 2023.
- [23] Y.-H. Zhu, X.-Z. Tian, and J. Zheng, "Performance analysis of the binary exponential backoff algorithm for IEEE 802.11 based mobile ad hoc networks," in *Proc. IEEE Int. Conf. Commun. (ICC)*, Jun. 2011, pp. 1–6.